Medicinal Plant Biology

ARTICLE

Open Access

https://doi.org/10.48130/mpb-0026-0005

Medicinal Plant Biology **2026**, 5: e012

The *NAC043* transcription factor from *Angelica sinensis* (Oliv.) Diels regulates lignin biosynthesis

Jin-jin Zhang[1,2], Chun-fan Xiang[1,2], Le-song Li[1,2], Juan Wang[1,2], Jia-die He[1,2], Meng-fei Li[3], Mohammad Omar Faruque[4], Shengchao Yang[1,2,5], Ying Xiao[6*] and Yan Zhao[1,2*]

[1] *Key Laboratory of Medicinal Plant Biology of Yunnan Province, National & Local Joint Engineering Research Center on Germplasms Innovation & Utilization of Chinese Medicinal Materials in Southwest China, Yunnan Agricultural University, Kunming 650201, China*

[2] *Yunnan Characteristic Plant Extraction Laboratory, Kunming 650106, China*

[3] *State Key Laboratory of Aridland Crop Science/College of Agronomy, Gansu Agricultural University, Lanzhou 730070, China*

[4] *Ethnobotany and Pharmacognosy Lab, Department of Botany, University of Chittagong, Chattogram-4331, Bangladesh*

[5] *Yunnan Province Key Laboratory of Cross-Border Chinese Herbal Materials, Honghe University, Honghe 661100, China*

[6] *State Key Laboratory of Discovery and Utilization of Functional Components in Traditional Chinese Medicine, Institute of Chinese Materia Medica, Shanghai University of Traditional Chinese Medicine, Shanghai 201203, China*

* Correspondence: xiaoyingtcm@shutcm.edu.cn (Xiao Y); zhaoyankm@126.com (Zhao Y)

Abstract

Angelica sinensis (Oliv.) Diels is a valuable medicinal plant whose dried roots are widely used in traditional Chinese medicine for blood enrichment and nourishment. NAC transcription factors (TFs) are known to play central roles in plant growth, secondary metabolism, and lignin biosynthesis. Here, we identified 122 *AsNAC* TFs from the *A. sinensis* genome. Phylogenetic analysis using NAC proteins from *Arabidopsis thaliana*, combined with expression profiling, identified *AsNAC043* as a key candidate regulator. Subcellular localization confirmed that AsNAC043 localizes specifically to the nucleus, consistent with its function as a TF. We subsequently constructed an *AsNAC043*-overexpressing transgenic line in *A. sinensis* callus. Overexpression of *AsNAC043* resulted in a significant increase in lignin content. Transcriptomic analysis further revealed upregulation of several key lignin biosynthesis genes, including *AsCCR* and *AsCAD*s. Our results demonstrate that *AsNAC043* may promote lignin accumulation in *A. sinensis* by activating the expression of core lignin biosynthesis genes. These findings provide insight into the molecular mechanism of *AsNAC*-mediated lignin biosynthesis, and offer valuable targets and theoretical support for breeding high-quality *A. sinensis* varieties.

Citation: Zhang JJ, Xiang CF, Li LS, Wang J, He JD, et al. 2026. The *NAC043* transcription factor from *Angelica sinensis* (Oliv.) Diels regulates lignin biosynthesis. *Medicinal Plant Biology* 5: e012 https://doi.org/10.48130/mpb-0026-0005

Introduction

Angelica sinensis (Oliv.) Diels is a perennial herbaceous plant of the Apiaceae family. Its dried root is commonly used in Chinese herbal medicine, rich in bioactive compounds such as organic acids, polysaccharides, and essential oils[1,2]. It is well recognized for its functions of enriching blood, promoting blood circulation, regulating menstruation, relieving pain, and moistening the intestines. It is considered a 'sacred herb for blood disorders', and a 'sacred herb for gynecological conditions', in folk medicine[3]. *A. sinensis* thrives in cool, shady, and humid environments at altitudes of 2,200–3,000 m and is intolerant to high temperatures. Its production is concentrated in southeastern Gansu Province, which is the main production area of the Taoist medicinal herbs[4], as well as in Yunnan, Sichuan, Hubei, and Shanxi Provinces. Premature bolting in *A. sinensis,* a common root medicinal plant in the Apiaceae family, leads to increased root lignification and the decomposition of numerous bioactive components, which eventually reduce the yield and quality of the medicinal material [5,6].

NAC transcription factors (TFs) play a key role in the biosynthesis of lignin in plants. They regulate lignin biosynthesis and deposition by directly or indirectly modulating the expression of downstream target genes, including essential enzymes in the phenylpropanoid pathway. Additionally, NAC TFs are involved in cell wall formation, secondary growth, and stress responses[7]. For example, in some plants, NAC TFs directly activate key lignin biosynthesis genes (e.g., *PAL*, *C4H*, *4CL*, *CCR*, and *CAD*). In *Capsicum annuum*, *CaNAC76* selectively binds to the promoter of *CaCAD1* to activate its transcription, thereby increasing lignin content and enhancing cold tolerance[8]. In rice, *OsNAC28* directly activates *CAD8B* and positively regulates lignin accumulation[9], while *OsNAC5* promotes lignin deposition by activating *OsCCR10*, thereby enhancing drought tolerance[10]. In the medicinal plant *Angelica dahurica,* recent studies have found that *AdNAC20* has a unique dual regulatory function. It not only regulates the biosynthesis of lignin, but also negatively regulates the accumulation of coumarin, a medicinal component. Transcriptome analysis predicts that *AdNAC20* can directly bind to the promoters of target genes containing SNBE-like motifs, such as *MYB46*, *C3H*, and *CCoAOMT*, which all have SNBE-like motifs, to regulate their transcription expression. This mechanism contributes to balancing lignification and secondary metabolism during *A. dahurica* premature bolting process[11]. Therefore, modulating *NAC* gene expression offers a promising approach for precisely controlling lignin content and composition, facilitating the breeding of stress-resistant varieties, and enhancing the potential applications of plants in bioenergy, papermaking, and agricultural quality improvement.

NAC TFs are known for their involvement in various biological processes, including plant growth, development, stress responses, and as metabolic pathways[12,13]. A notable number of research studies on NAC TFs have been reported in *A. thaliana*[14], *Populus tomentosa*[15], *Camellia sinensis*[16], *Triticum aestivum*[17], and *O. sativa*[18], as well as in medicinal plants such as *Panax notoginseng*[19], *Eleutherococcus senticosus*[20], and *Panax ginseng*[21].

However, the role of NAC TFs in regulating lignin biosynthesis in *A. sinensis* is still ambiguous. In this study, we identified the NAC TFs family in *A. sinensis* and determined the key candidate gene *AsNAC043* through phylogenetic analysis. Additionally, we constructed an *AsNAC043* overexpression vector and performed functional validation using a native callus transformation system in *A. sinensis*. Our objective was to investigate the effect of the *AsNAC043* TF on lignin accumulation in *A. sinensis* roots, and to provide a foundation for elucidating the molecular regulatory mechanism of root lignification in this species. The findings of this study will enhance the theoretical understanding of secondary metabolism regulation in medicinal plants, and provide new strategies and targets for their genetic improvement.

Materials and methods

Plant materials, strains, and plasmids

A. sinensis plants were cultivated in She Block Township, Dongchuan District, Kunming City, Yunnan Province (latitude 26°15′7″ N, longitude 102°57′15″ E, altitude 3,254.46 m). The specimens were identified as *A. sinensis* (Oliv.) Diels (Apiaceae) by researcher Wenguang Yang (Kunming Institute of Botany, Chinese Academy of Sciences), and deposited at the Kunming Institute of Botany (voucher no. 20231019). The roots of *A. sinensis* bolting plants (BP) and unbolting plants (UBP) were collected in September 2022, quick-frozen in liquid nitrogen, and stored at −80 °C for spare use. *Nicotiana benthamiana* seeds were placed in sterile water and cold treated at 4 °C for 12 h before being sown into nutrient soil. Cultivation was accomplished in a greenhouse maintained at 23 °C. Once seedlings had develop four true leaves, they were transplanted with soil into pre-dug holes, and cultivation was continued in the 23 °C greenhouse.

Escherichia coli DH5α competent cells were purchased from Sangon Biotech (Shanghai) Co., Ltd. *Agrobacterium tumefaciens*: GV3101 competent cells were purchased from Beijing TransGen Biotech Co., Ltd. Plants expression vector pCAMBIA1300-GFP was maintained in our laboratory for future use.

Callus induction of *A. sinensis*

Sterile seedlings of *A. sinensis* were inoculated onto 1/2 MS medium (pH = 5.8) supplemented with 30 g/L sucrose, 4 g/L agar, 2 mg/L 3-indolebutyric acid (IBA), 0.2 mg/L kinetin (KT), and 0.5 g/L activated carbon to induce callus formation. The resulting callus tissue was then transferred to 1/2 MS medium (pH = 5.8) containing 20 g/L sucrose, 8 g/L agar, 2 mg/L IBA, and 0.5 g/L activated carbon to promote shoot formation. The induction of aseptic seedlings, callus, and shoot calli were all carried out in a culture room at 17 °C.

Identification of NAC family members and construction of expression profiling

Genome and annotation files of *A. sinensis* were retrieved from the NCBI database[22]. Transcriptome sequencing data were assembled based on the reference genome. The Pfam ID PF02365 for the NAC domain was downloaded from the UniProt database, and the corresponding Pfam feature file was obtained from Pfam (http://pfam.xfam.org/search). Candidate sequences containing the NAC domain were extracted using the 'HMM Search' tool in TBtools-II v2.154, with an E-value cutoff of $< 1 \times 10^{-5}$. in the domain scores. The CDS and protein sequences of NAC members were extracted using the 'Fasta Extract' tool in TBtools. Redundant or incomplete sequences were manually removed, retaining only those with complete NAC domains. Known functional NAC sequences from *A. thaliana* were downloaded from the TAIR database (www.arabidopsis.org/), and a phylogenetic tree was constructed using the neighbor-joining method. A heatmap was generated based on the normalized TPM values of 12 candidate *NAC* genes using the 'Heatmap' tool in TBtools.

Physicochemical properties and chromosomal localization analysis of the AsNAC gene family

TBtools was employed to explore the physicochemical properties of the proteins encoded by the *A. sinensis* NAC gene family, along with amino acid number, molecular weight, theoretical pI, instability index, aliphatic index, and grand average of hydropathicity (GRAVY). Likewise, the WoLF PSORT online tool was used to predict subcellular localization. Chromosomal localization information for the *AsNAC* genes was obtained from the GFF3 genome annotation file in the NCBI database, which was then displayed using TBtools[23,24].

Analysis of conserved motifs, domains, and gene structure

Conserved motifs in the AsNAC protein sequences were identified using the MEME online tool (https://meme-suite.org/meme/tools/meme), with the number of motifs set to 10, and all other parameters set as default values (where the basic sequence width ranges from 6 to 50). Domain information obtained from the CDD database was integrated with motif data. A phylogenetic tree was constructed using the neighbor-joining method in MEGAX64. TBtools was used to visualize the exon-intron structures, conserved motif distributions, and domain architectures of the AsNAC proteins[25].

RNA extraction and cloning of the *AsNAC043* gene

Root tissue samples were collected from BP and UBP of *A. sinensis*. The tissue was ground in liquid nitrogen, and total RNA was extracted using the HiPure Plant RNA Mini Kit (Guangzhou Meiji Biotechnology Co., Ltd). RNA quality was assessed according to the manufacturer's instructions, and high-quality RNA samples were selected for subsequent experiments. cDNA was synthesized from the selected RNA using Hifair® AdvanceFast 1st Strand cDNA Synthesis Kit and stored at −20 °C. Based on the *AsNAC043* gene sequence, specific gene cloning primers were designed (Supplementary Table S1). The coding sequence (CDS) of the *AsNAC043* gene was cloned and analyzed by agarose gel electrophoresis. Results indicated that the cloned *AsNAC043* gene ranged between 1,000 bp and 1,500 bp in length, consistent with the expected size. Subsequently, the gel was recovered (Supplementary Fig. S1).

Construction of plant expression vectors.

The expression vector pCAMBIA1300 was digested by the restriction enzyme *BamH*I. The digested plasmid was purified using the omega E.Z.N.A.® Cycle-Pure Kit column purification system. Under the catalysis of seamless cloning enzymes, the target gene was connected to the digested plasmid at 50 °C for 50 min. After the reaction, the recombinant product was transformed into the competent cells of *E. coli* DH5α. The activated cells were inoculated on LB solid medium containing 100 mg/L kanamycin, and cultured

at 37 °C for 12–14 h. Choosing a colony for PCR verification, the PCR-positive colonies were placed in LB liquid medium containing kanamycin and cultured overnight at 37 °C and 200 rpm. Plasmids were extracted and sequenced. Finally, according to the sequencing results, it was determined whether the target gene has been successfully integrated into the vector.

Confocal laser scanning microscope (CLSM) analysis

The pC1300-GFP empty vector stored in the laboratory, and the pC1300-*AsNAC043*-GFP recombinant plasmid successfully sequenced, were transfected into competent cells of *A. tumefaciens* GV3101, which was then incubated at 30 °C and 200 rpm for 2–3 h. The activated bacteria was spread onto an LB solid medium containing 100 mg/L kanamycin and incubated at 30 °C for 48 h. A positive colony was chosen and inoculated into a 6 mL LB liquid culture medium containing kanamycin, and cultured at 30 °C and 200 rpm for 24 h. Then, 700 μL of the bacterial suspension was mixed with 700 μL of 50% glycerol and stored at −80 °C. The remaining culture was transferred to 30 mL LB medium containing kanamycin and amplified to an OD_{600}, reaching 0.6–0.8. The bacterial cells were centrifuged at 1,000 rpm for 5 min, and the supernatant was discarded. The pellet was resuspended in a solution containing 10 mM MES, 1 mM $MgCl_2$, and 150 μM acetosyringone (AS), and incubated for 0.5–3 h. The bacterial suspension was then gently injected into the lower epidermis of tobacco leaves using a needle without a tip. After injection, the tobacco plants were kept in the dark for 12–15 h, then transferred to suitable environmental conditions for 24 h[26]. The lower epidermis of the injected leaves was peeled off, placed on a slide, flattened, and stained with the nuclear dye DAPI. Fluorescence imaging was performed using a laser confocal microscope.

Agrobacterium tumefaciens-mediated stable transformation of *A. sinensis* callus

Ten microliter of *A. tumefaciens* stored in a −80 °C freezer and inoculate it into 6 mL of LB liquid medium containing kanamycin. It was then cultured at 30 °C and 200 rpm for 24 h, then transfer to 30 mL of LB medium containing kanamycin for culture expansion. When the OD_{600} reached 0.3–0.4, the bacterial cells were collected by centrifugation. Bacterial cells were collected by centrifugation and resuspended in an MS medium containing 100 μmol/L acetosyringone. After dark incubation for 30 min, 20-d-old *A. sinensis* callus was immersed in the bacterial suspension for 8–10 min, blotted dry on filter paper, and transferred to MS co-culture medium (pH = 5.8), containing 15 g/L sucrose, 7 g/L agar, 0.5 g/L activated carbon, and 100 μmol/L AS. After 2 d of dark co-culture, the callus was transferred to a selection medium consisting of 1/2 MS medium (pH = 5.8), supplemented with 20 g/L sucrose, 8 g/L agar, 2 mg/L IBA, 0.5 g/L activated carbon, 25 mg/L kanamycin, and 270 mg/L Timentin[27,28]. The medium was replaced weekly for 2 to 3 weeks until clear differentiation and growth of callus tissue were observed. Positive transformants were identified by PCR.

RT-qPCR analysis

Total RNA was extracted from positive *A. sinensis* callus tissue and reverse-transcribed into cDNA using the PrimeScript™ RT Reagent Kit with gDNA Eraser (RR047A, Takara). The cDNA was stored at −20 °C. RT-qPCR was performed using Novazene's AceQ qPCR SYBR Green Master Mix according to the manufacturer's instructions. Primers are listed in Supplementary Table S1. The *AsEEF1G* gene was used as an internal reference[29]. The reaction system was prepared according to the F488 SYBR qPCR Mix manual, with the following cycling program: 95 °C for 30 s, 40 cycles of 95 °C for 15 s, and 60 °C for 20 s; followed by 95 °C for 15 s, 60 °C for 1 min, and 95 °C for 15 s. Three biological replicates and four technical replicates were performed, excluding outliers. Relative gene expression was calculated using the $2^{-\Delta\Delta CT}$ method.

Determination of lignin content

Comin lignin content determination kit (Cat No. MZS-2-G, Suzhou Keming Biotechnology Co., Ltd, China) was used to determine the lignin content in plant samples according to the kit instructions[30]. A 4:1 (v/v) mixture of acetic acid/acetyl bromide was mixed with approximately 5 mg of dry samples, thereafter incubated at 80 °C for 40 min, shaken every 10 min, and allowed to cool at room temperature. A 1:1 (v/v) mixture of 2 M NaOH/acetic acid was added to stop the reaction. A spectrophotometer (Hitachi SU1000) was employed to measure the extracted lignin from the supernatant of each sample at 280 nm. A standard curve ($y = 0.0347x + 0.0068$, $R^2 = 0.9889$) was used to calculate the total lignin content. The calculation was performed with the formula: lignin (mg/g) = $(0.0294 \times [\Delta A - 0.0068])/W \times T$, where W represents the sample weight (g), T represents the dilution ratio, and ΔA represents the absorbance value obtained by applying the spectrophotometric values using the standard curve. The lignin percentage content (%) is then calculated as: lignin percentage (%) = (lignin content [mg/g]/1,000) × 100%, a unit conversion factor of 1,000 is applied (since 1 g = 1,000 mg)[31].

RNA-seq and DEGs analysis

Raw reads were processed with fastp (v0.18.0)[32] to remove adapter sequences, reads with > 10% unknown nucleotides (N), and reads with > 50% low-quality bases (Q ≤ 20). Clean reads were aligned to the reference genome using HISAT2.2.4[33] with default parameters. Gene annotation was performed by aligning sequences to the KEGG (www.genome.jp/kegg/), NR, GO, and KOG databases using BLAST (https://blast.ncbi.nlm.nih.gov/Blast.cgi). Differentially expressed genes (DEGs) analysis was conducted with DESeq2, with DEGs defined as those with FDR < 0.05, and $|\log_2(\text{fold change})| \geq 2$. Expression levels were quantified as TPM values using RSEM.

Statistical analysis

This study employed a one-factor experimental design with three independent biological replicates per treatment group. Data are presented as mean ± standard deviation (SD), and one-way analysis of variance (ANOVA) was performed using GraphPad Prism 10.3 software to test for intergroup differences[34].

Results

Identification and characterization of the *A. sinensis* NAC gene family

A total of 122 AsNAC family members were identified from the reference genome of *A. sinensis*. Sequence analysis indicated that the CDS lengths ranged from 351 to 3,195 bp, encoding proteins of 116 to 1,064 amino acids. Analysis of physicochemical properties using TBtools revealed that the molecular weights of the AsNAC

proteins ranged from 13.6258 to 120.73788 kDa, and their theoretical isoelectric points varied from 4.35 to 9.96, indicating that this protein family exhibits both basic and acidic characteristics, with most members being predominantly acidic proteins (Supplementary Table S2). Using WoLF PSORT, subcellular localization predictions showed that 72.13% (88 out of 122) of *AsNAC* genes are localized in the nucleus, indicating a predominant role in regulating plant growth and development. The remaining members were distributed in the cytoplasm, chloroplasts, and peroxisomes. Chromosomal localization analysis revealed that the 122 *AsNAC* genes are distributed across all 11 chromosomes, with two additional genes located in scaffold regions (Supplementary Fig. S2).

Conserved motifs, domains, and gene structures of *A. sinensis* NACs

TBtools software was used to analyze conserved motifs, domains, and gene structures of 122 *A. sinensis* NAC proteins. Ten conserved motifs, designated motif 1 to motif 10, and consisting of 11 to 50 residues were identified (Supplementary Figs S3a, S4). Motif 6 was the most frequent and represents the core conserved motif of the family, whereas motif 9 was the least common. The composition and arrangement of motifs varied considerably among different evolutionary clades, although members within the same clade generally exhibited similar motif patterns, implying functional conservation. All 122 AsNAC proteins contained the typical no-apical-meristem (NAM) domain, with AS06G02092 additionally harboring a CRS1-Yhby domain (Supplementary Fig. S3b). Gene structure analysis showed that *AsNAC* genes contain 0–3 introns, and 1–9 exons (Supplementary Fig. S3c). Overall, genes within the same evolutionary branch displayed similar structural features, supporting the evolutionary conservation of the AsNAC family in *A. sinensis*.

Phylogenetic and expression pattern analysis of *A. sinensis* NACs

To investigate the phylogenetic relationships of the AsNAC family, a phylogenetic tree was constructed using 122 *A. sinensis* and 105 *A. thaliana* NAC protein sequences (Fig. 1a). The AsNAC members were classified into 18 subfamilies, all of which contained representatives from both species. In the OsNAC7 subfamily, genes such as *AS02G00175*, *AS01G01899*, and *AS05G01615* clustered with *A. thaliana ANAC043* and *ANAC012*. In the NAP subfamily, AS10G00848 and ANAC029 formed a distinct branch. This clustering pattern suggests that NAC proteins from the two species with high sequence similarity may perform analogous functions. Given that *A. thaliana ANAC043* (in the OsNAC7 subfamily) is involved in lignin biosynthesis, we hypothesized that its orthologs in *A. sinensis*, including *AS02G00175*, may also regulate lignin synthesis. Expression analysis of 12 *AsNAC* genes from the OsNAC7 subfamily revealed that *AS02G00175* was most significantly upregulated in BP[31] (Fig. 1b). Therefore, we have renamed *AS02G00175* to *AsNAC043* as a candidate gene for subsequent functional validation.

Cloning and subcellular localization of *AsNAC043*

In this study, the DNA sequence of *AsNAC043* was cloned from *A. sinensis*. The full length of the sequence is 1,266 bp, encoding 422 amino acids, including five subdomains (A–E) at the N- terminal (Supplementary Fig. S5).

To further elucidate the subcellular localization of the AsNAC043, we used *A. tumefaciens* transient transformation. *A. tumefaciens* carrying the empty vector pC1300-GFP, and the fusion expression vector pC1300-*AsNAC043*-GFP were injected into *N. benthamiana* leaves, respectively, to realize the instantaneous expression of the target gene. Confocal imaging showed that GFP signals from the control were distributed throughout the cell, including the membrane and nucleus. In contrast, the AsNAC043-GFP fusion protein was exclusively localized in the nucleus (Fig. 2), consistent with its predicted function as a TF.

Functional characterization of *AsNAC043* gene in *A. sinensis*

The *AsNAC043* gene fragment was connected to the pC1300 vector and transformed. PCR analysis of the single colony confirmed

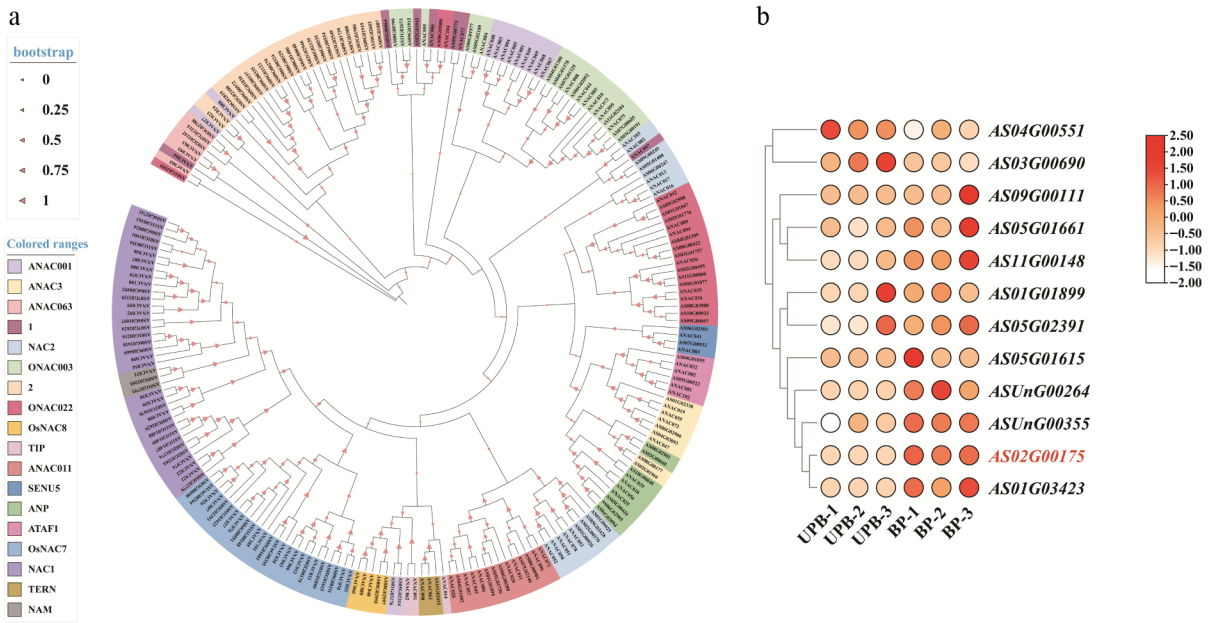

Fig. 1 Phylogenetic and expression analysis of NAC TFs in *A. sinensis*. (a) Phylogenetic tree of *A. sinensis* NAC TFs. (b) Expression pattern of OsNAC7 subfamily.

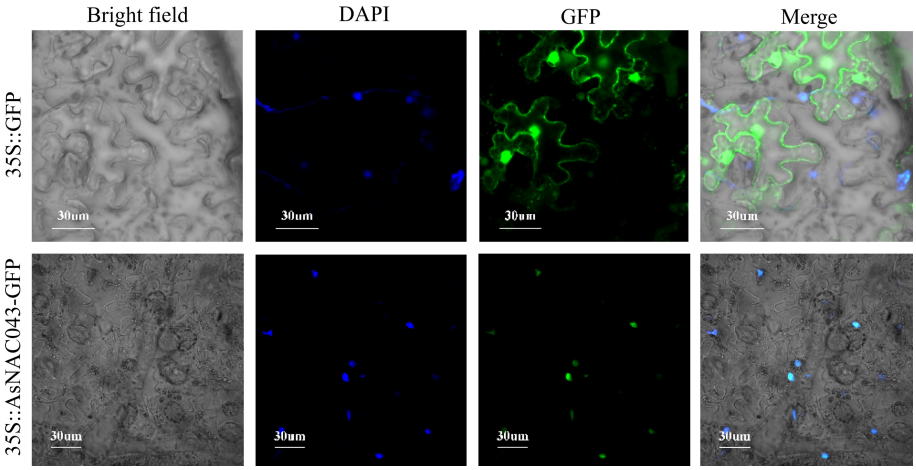

Fig. 2 Subcellular localization of *AsNAC043* in lower epidermal cells of *N. benthamiana* leaves.

that *AsNAC043* was successfully recombined with the pC1300 vector. (Supplementary Fig. S6). The recombinant plasmid was introduced into *A. tumefaciens* GV3101 and used to transform *A. sinensis* callus.

After 3 to 4 weeks of subculture, transgenic lines (OE1, OE2, OE3) showed slower growth compared to wild-type (WT) plants. RT-qPCR analysis confirmed that *AsNAC043* expression was significantly increased in the OE lines (Fig. 3a, b). Given the potential role of *AsNAC043* in lignin biosynthesis, total lignin content was measured. UV spectrophotometric analysis revealed a significant increase in lignin content in the *AsNAC043*-overexpressing callus tissues compared to the WT (Fig. 3c).

RNA-seq analysis of *AsNAC043*-overexpressing plants

To explore the global transcriptional changes induced by *AsNAC043* overexpression, RNA-seq was performed on WT and OE callus tissues with three biological replicates per group. Principal component analysis (PCA) clearly separated the WT and OE samples, and correlation heatmaps indicated high reproducibility among replicates (Fig. 4a, b). A total of 6,885 DEGs were identified, including 2,594 upregulated and 4,291 downregulated genes (Fig. 4c, d, Supplementary Table S3). GO enrichment analysis assigned the DEGs in terms of biological process, molecular function, and cellular component categories. KEGG pathway analysis indicated that the DEGs were predominantly enriched in pathways related to secondary metabolite biosynthesis, phenylpropanoid biosynthesis, metabolic pathways, and flavonoid biosynthesis (Fig. 4e, f).

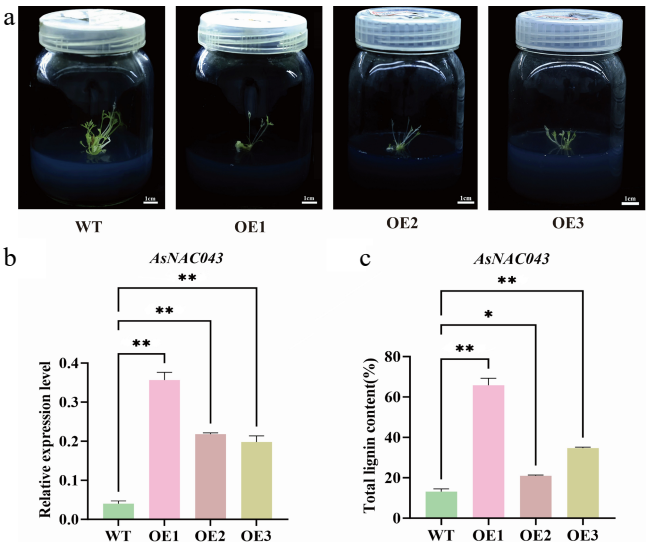

Fig. 3 Characterization of WT and *AsNAC043*-overexpressing transgenic lines (*AsNAC043*-OE). (a) Phenotypes of WT and *AsNAC043*-OE in *A. sinensis* plants. OE1, OE2, and OE3 represent independent transgenic lines. (b) RT-qPCR analysis of *AsNAC043* expression in WT and transgenic lines (OE1, OE2, OE3). (c) Lignin content in WT and transgenic plants. An asterisk indicates a significant difference (* $p < 0.05$; ** $p < 0.01$).

Effects of *AsNAC043* overexpression on lignin synthesis-related genes and protein interaction networks

Transcriptome data were used to analyze the expression of *AsNAC043* and key lignin biosynthesis genes. Results indicate that the expression level of the *AsNAC043* gene is significantly upregulated in the OE line, as well as key lignin pathway genes such as *AsCCR* (*AS07G02794*), and *AsCADs* (*AS01G01636*, *AS01G00171*, *AS06G03766*). Phenylpropanoid pathway genes, including *AsPALs* (*AS06G01386*, *AS05G03296*), and *As4CLs* (*AS06G02531*, *AS07G02833*), were also upregulated. In contrast, genes involved in ferulic acid biosynthesis (*AsCOMT*, *AS01G03183*), and flavonoid synthesis (*AsCHI, AS03G00525*) were downregulated. Among TFs, *AsMYB* (*AS09G01066*) was upregulated, while *AsMYB* (*AS10G02150*) and *AsF5H* (*AS04G00561*) were downregulated (Fig. 5a).

Protein interaction network analysis revealed that MYB TFs (AS09G01066, AS10G02150) interact with key lignin biosynthesis genes such as *CCR*, *CADs*, *COMT*, *4CL*, *PAL*, and *F5H*. AsNAC043 also showed strong associations with AsMYBs, AsF5H, and AsCCR, suggesting close regulatory relationships and potential synergy in the regulation of lignin biosynthesis (Fig. 5b).

Discussion

Recently, with the expanding market demand for root and rhizome medicinal ingredients, many plants are prone to premature bolting and flowering during cultivation due to germplasm degradation, nutrient accumulation, and external environmental influences. Since the medicinal properties of these plants are predominantly found in their roots or rhizomes, premature

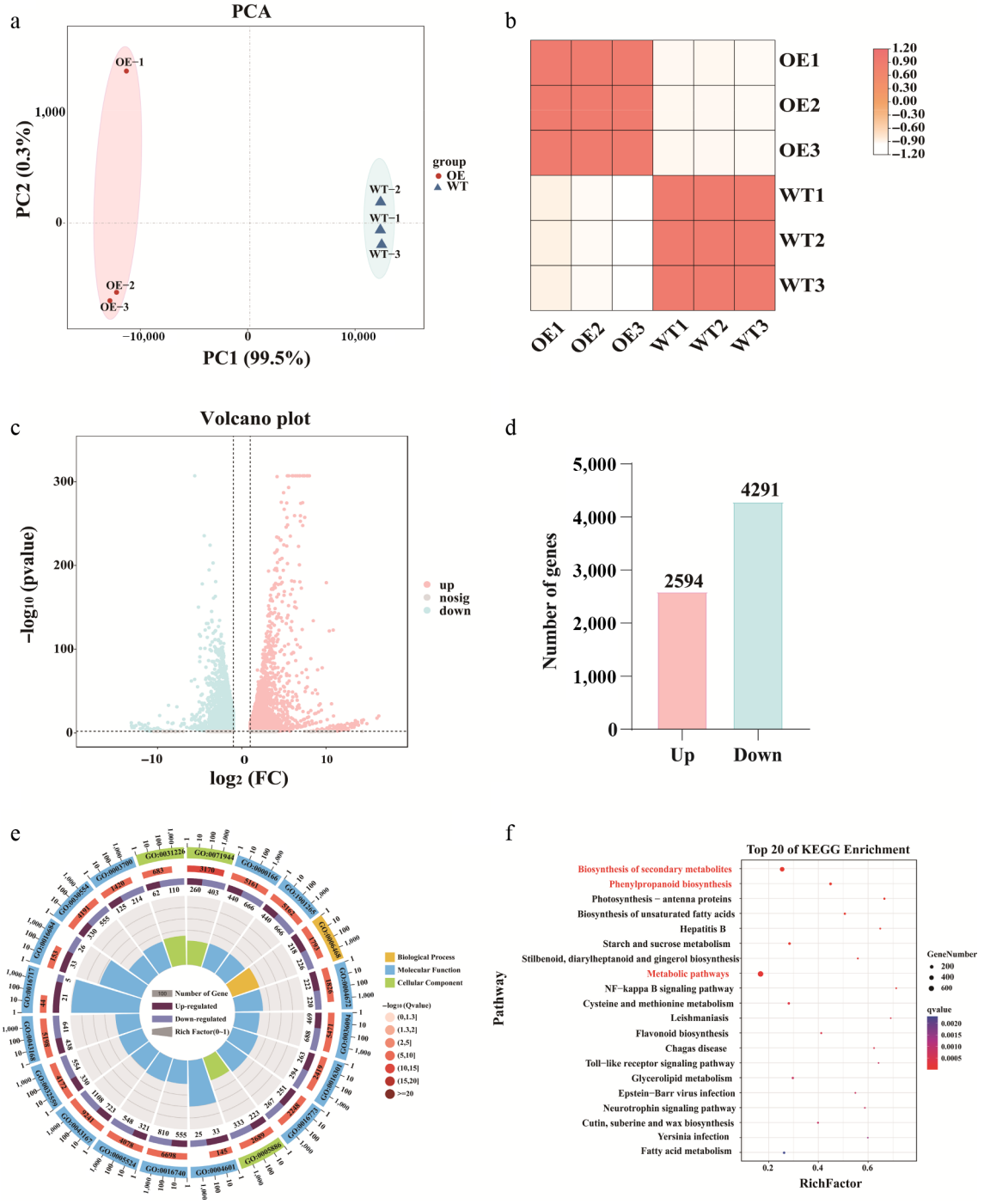

Fig. 4 Differential gene expression and enrichment analysis of WT and *AsNAC043*-overexpressing transgenic lines (*AsNAC043*-OE). (a) Principal component analysis (PCA). (b) Sample correlation analysis. (c) Volcano plot of differential expressed genes. (d) Statistics of differentially expressed genes. (e) GO functional enrichment analysis. (f) KEGG pathway enrichment analysis.

flowering disrupts nutrient allocation, accelerates root lignification, and severely compromises both the quantity and quality of the crude drug[6]. Previous studies have demonstrated a close association between TFs and lignin biosynthesis in plants (Supplementary Table S4). For instance, a NAC TF (LOC107435239) was identified in *Ziziphus jujuba* Mill that upregulates *F5H* expression, thereby promoting lignin accumulation[35]. Lignification in Pyrus fruit is regulated by *PpNAC187*, where the overexpression of *PpNAC187* upregulates *CCR* and *COMT* gene expression, thereby increasing lignin content[36]. Overexpression of *OsNAC17* in *O. sativa* induces lignin-related gene expression, promotes lignin accumulation in leaves and roots, and enhances drought tolerance[37]. Similarly, in *Eucalyptus grandis*[38] and *Apium graveolens*[39], heterologous or homologous overexpression of *NAC* genes effectively activates the lignin synthesis pathway, thereby increasing lignin accumulation levels in plants.

This study identified 122 members of the AsNAC family in *A. sinensis*. Subcellular localization predictions indicated that 72.13% of AsNAC proteins are nuclear-localized, aligning with the canonical role of NAC TFs in transcriptional regulation. The localization of a subset of

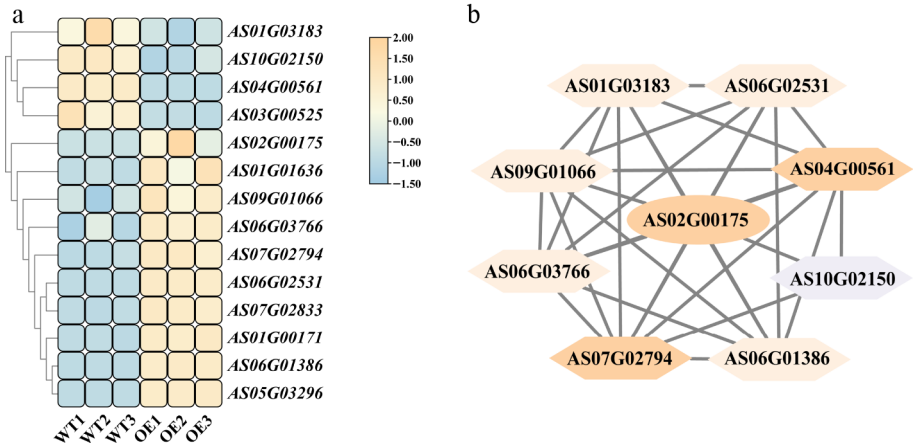

Fig. 5 Effects of *AsNAC043* overexpression on the expression of lignin biosynthesis-related genes and protein interaction network analysis. (a) Heatmap of key lignin biosynthesis gene expression in the WT and *AsNAC043*-OE lines. (b) Analysis of the Interaction network among proteins encoded by key genes in lignin biosynthesis. *AsNAC043* (AS02G00175); *AsPALs* (AS06G01386, AS05G03296); *AsCADs* (AS01G00171, AS06G03766, AS01G01636); *As4CLs* (AS06G02531, AS07G02833); *AsCCR* (AS07G02794); *AsCOMT* (AS01G03183); *AsCHI* (AS03G00525); *AsF5H* (AS04G00561), and *AsMYBs* (AS09G01066, AS10G02150).

AsNAC proteins to the cytoplasm, chloroplasts, and peroxisomes suggests potential roles in signal transduction or organelle-specific functions, possibly mediated by dynamic subcellular redistribution. Such diversity in localization has also been observed in NAC families of other plants, including *Miscanthus sinensis*[40], highlighting the functional complexity of this gene family. The 122 *AsNAC* genes were predominantly distributed across 11 chromosomes, with two genes located in scaffold regions. This distribution may reflect evolutionary occurrences such as segmental or tandem duplications, which could potentially lead to functional diversification. All AsNAC proteins possess the conserved NAM domain[41,42], thereby validating the reliability of our identification. The presence of an additional CRS1-Yhby domain in some members may confer specialized functions, warranting further investigation.

To further identify key NAC members involved in lignification, we performed phylogenetic and expression analysis and identified *AsNAC043*, an ortholog of *A. thaliana ANAC043*[43]. Using *A. tumefaciens*-mediated transformation, we successfully overexpressed *AsNAC043* in *A. sinensis* callus. RT-qPCR confirmed significantly increased *AsNAC043* expression in transgenic lines (OE1, OE2, OE3) compared to WT, establishing a reliable system for functional studies. Lignin content assays revealed a significant elevation in total lignin within *AsNAC043*-OE calli, indicating that *AsNAC043* positively regulates lignin biosynthesis. Protein interaction network analysis revealed that AsNAC043 not only interacts with genes associated with lignin biosynthesis, but also exhibits particularly strong associations with MYB TFs. Previous studies have demonstrated that *Pyrus WRKY46* can directly activate the transcription of *NAC187*, thus promoting the expression of the lignin biosynthesis gene *CCR* and enhancing lignin accumulation[44]. It is also found that PbNAC47 forms complexes with PbAGL7 and PbMYB73, forming complexes that synergistically activate target genes and promote lignin biosynthesis and secondary wall thickening in stone cells[45]. Overexpression of *CgNAC043* in *Citrus grandis* directly activates the promoters of *CgMYB46*, *CgCCoAOMT*, and *CgC3H*, upregulates *CgMYB58* expression, and enhances lignin accumulation in vacuoles[43]. Therefore, it can be inferred that AsNAC043 may also form regulatory complexes with MYB TFs (e.g., AS06G02257, and AS04G00182) to synergistically enhance the expression of lignin-related genes and improve regulatory efficiency.

To elucidate the molecular mechanisms underlying *AsNAC043*-mediated lignin biosynthesis, we conducted RNA-seq analysis of WT and *AsNAC043*-OE callus. Principal component analysis clearly separated the WT and OE groups, revealing 6,885 DEGs, which signifies that *AsNAC043* overexpression substantially alters the transcriptome. GO and KEGG enrichment analyses showed that DEGs were significantly enriched in pathways related to secondary metabolite biosynthesis, phenylpropanoid biosynthesis, metabolic pathways, and flavonoid biosynthesis, suggesting that *AsNAC043* modulates lignin synthesis through these metabolic pathways. Specifically, the expression of key lignin biosynthesis genes *AsCCR* and *AsCADs*, along with phenylpropanoid pathway genes *AsPALs* and *As4CLs*, was significantly upregulated in OE lines. In contrast, genes involved in ferulic acid biosynthesis (*AsCOMT*) and flavonoid synthesis (*AsCHI*) were downregulated. This result indicates that *AsNAC043* may positively regulate the phenylpropanoid pathway to redirect metabolic flux toward the lignin biosynthesis branch while simultaneously inhibiting the flavonoid biosynthesis pathway, a competing metabolic route. The downregulation of *AsCOMT* may be related to the stage-specific characteristics of lignin biosynthesis and the functional bias of metabolic branches.

Overall, *AsNAC043* acts as a positive regulator of lignin biosynthesis in *A. sinensis*, likely through direct activation of lignin pathway genes, and suppression of alternative metabolic pathways. These insights enhance our understanding of the transcriptional network controlling lignin biosynthesis in *A. sinensis,* and establish a theoretical foundation for improving medicinal quality by genetic engineering. Future work should focus on validating direct target genes of *AsNAC043* and exploring its potential roles in plant development and stress responses.

Conclusions

In conclusion, this study successfully identified and characterized the NAC TFs family in *A. sinensis*, with a particular focus on *AsNAC043*. Our findings demonstrate that AsNAC043 localizes to the nucleus and functions as a positive regulator of lignin biosynthesis. Overexpression of *AsNAC043* in transgenic calli led to significantly increased lignin content and altered expression of key genes in the lignin biosynthesis pathway. Transcriptome analysis further revealed

that *AsNAC043* regulates multiple metabolic pathways, including phenylpropanoid biosynthesis, while repressing competing pathways such as flavonoid biosynthesis. These results not only provide important insights into the molecular mechanisms underlying lignin accumulation in *A. sinensis,* but also offer valuable genetic targets for future breeding strategies aimed at improving medicinal quality through reduced root lignification.

Author contributions

The authors confirm their contributions to the paper as follows: experimentation, data analysis, mapping, manuscript drafting and revision: Zhang JJ, Xiang CF, Li LS, Wang J, He JD; revised the manuscript: Li MF, Faruque MO, Yang S; conceived and designed the experiments, and wrote and revised the manuscript: Xiao Y, Zhao Y. All authors reviewed the results and approved the final version of the manuscript.

Data availability

All data generated or analyzed during this study are included in this published article and its supplementary information files.

Acknowledgments

This work was supported by the National Natural Science Foundation of China (82460743), the Major Special Science and Technology Project of Yunnan Province (202502AS100012; 202403AK140082), Yunnan Characteristic Plant Extraction Laboratory (2022YKZY001), Yunnan Province Youth Talent Support Program (XDYC-QNRC-2022-0219), the National Key Research and Development Program of China (2023YFC3504800), and Program of Shanghai Academic/Technology Research Leader (23XD1423500).

Conflict of interest

The authors declare that they have no known competing financial interests or personal relationships that could have appeared to influence the work reported in this paper.

Supplementary information accompanies this paper online at: https://doi.org/10.48130/mpb-0026-0005.

Dates

Received 7 December 2025; Revised 2 February 2026; Accepted 11 March 2026; Published online 26 May 2026

References

[1] Wei WL, Zeng R, Gu CM, Qu Y, Huang LF. 2016. *Angelica sinensis* in China – a review of botanical profile, ethnopharmacology, phytochemistry and chemical analysis. *Journal of Ethnopharmacology* 190:116–141

[2] Ma JP, Guo ZB, Jin L, Li YD. 2015. Phytochemical progress made in investigations of *Angelica sinensis* (Oliv.) Diels. *Chinese Journal of Natural Medicines* 13:241–249

[3] Su KH, Su SY, Ko CY, Cheng YC, Huang SS, et al. 2021. Ethnopharmacological survey of traditional Chinese medicine pharmacy prescriptions for dysmenorrhea. *Frontiers in Pharmacology* 12:746777

[4] Zhang HY, Bi WG, Yu Y, Liao WB. 2012. *Angelica sinensis* (Oliv.) Diels in China: distribution, cultivation, utilization and variation. *Genetic Resources and Crop Evolution* 59:607–613

[5] Han X, Li M, Yuan Q, Lee S, Li C, et al. 2023. Advances in molecular biological research of *Angelica sinensis*. *Medicinal Plant Biology* 2:16

[6] Liu X, Luo M, Li M, Wei J. 2022. Depicting precise temperature and duration of vernalization and inhibiting early bolting and flowering of *Angelica sinensis* by freezing storage. *Frontiers in Plant Science* 13:853444

[7] Zhao Y, Liu G, Yang F, Liang Y, Gao Q, et al. 2023. Multilayered regulation of secondary metabolism in medicinal plants. *Molecular Horticulture* 3:11

[8] Xiao J, Sui X, Xu Z, Liang L, Tang W, et al. 2025. CaNAC76 enhances lignin content and cold resistance in pepper by regulating CaCAD1. *International Journal of Biological Macromolecules* 285:138271

[9] Yuan DP, Yang S, Feng L, Chu J, Dong H, et al. 2023. Red-light receptor phytochrome B inhibits BZR1-NAC028-CAD8B signaling to negatively regulate rice resistance to sheath blight. *Plant, Cell & Environment* 46:1249–1263

[10] Bang SW, Choi S, Jin X, Jung SE, Choi JW, et al. 2022. Transcriptional activation of rice *CINNAMOYL-CoA REDUCTASE 10* by OsNAC5, contributes to drought tolerance by modulating lignin accumulation in roots. *Plant Biotechnology Journal* 20:736–747

[11] Qu W, Huang W, Chen C, Chen J, Zhao L, et al. 2024. *AdNAC20* regulates lignin and coumarin biosynthesis in the roots of *Angelica Dahurica* var. *formosana*. *International Journal of Molecular Sciences* 25:7998

[12] Han K, Zhao Y, Sun Y, Li Y. 2023. NACs, generalist in plant life. *Plant Biotechnology Journal* 21:2433–2457

[13] Gao Q, Zhang J, Cao J, Xiang C, Yuan C, et al. 2024. MetaDb: a database for metabolites and their regulation in plants with an emphasis on medicinal plants. *Molecular Horticulture* 4:17

[14] Xu P, Ma W, Feng H, Cai W. 2024. The NAC056 transcription factor confers freezing tolerance by positively regulating expression of CBFs and NIA1 in *Arabidopsis*. *Plant Communications* 5:100923

[15] Han K, Zhao Y, Liu J, Tian Y, El-Kassaby YA, et al. 2024. Genome-wide investigation and analysis of NAC transcription factor family in *Populus tomentosa* and expression analysis under salt stress. *Plant Biology* 26:764–776

[16] Qiu S, Shao C, Xu R, Luo Y, Hu Q, et al. 2025. Identification of the NAC gene family in *Camellia sinensis* and expression analysis of *CsNAC65* under shading treatment. *Beverage Plant Research* 5:e024

[17] Mao H, Li S, Chen B, Jian C, Mei F, et al. 2022. Variation in *cis*-regulation of a NAC transcription factor contributes to drought tolerance in wheat. *Molecular Plant* 15:276–292

[18] Kim Y, Kim B, Kang J, Bae SI, Yoon H, et al. 2025. *ONAC005* enhances salt stress tolerance by promoting suberin deposition in root endodermis. *The Plant Journal* 123:e70469

[19] Zhang X, Huang Y, Shi Y, Wang X, Chen W, et al. 2025. PnNAC03 from *Panax notoginseng* functions in positively regulating saponins and lignin biosynthesis during cell wall formation. *Plant Cell Reports* 44:63

[20] Dong J, Zhao X, Song X, Wang S, Zhao X, et al. 2024. Identification of *Eleutherococcus senticosus* NAC transcription factors and their mechanisms in mediating DNA methylation of EsFPS, EsSS, and EsSE promoters to regulate saponin synthesis. *BMC Genomics* 25:536

[21] Jiang T, Zhang Y, Zuo G, Luo T, Wang H, et al. 2024. Transcription factor PgNAC72 activates *DAMMARENEDIOL SYNTHASE* expression to promote ginseng saponin biosynthesis. *Plant Physiology* 195:2952–2969

[22] Han X, Li C, Sun S, Ji J, Nie B, et al. 2022. The chromosome-level genome of female ginseng (*Angelica sinensis*) provides insights into molecular mechanisms and evolution of coumarin biosynthesis. *The Plant Journal* 112:1224–1237

[23] Chen C, Wu Y, Li J, Wang X, Zeng Z, et al. 2023. TBtools-II: a 'one for all, all for one' bioinformatics platform for biological big-data mining. *Molecular Plant* 16:1733–1742

[24] Arshad KT, Li C, Li L, Wang J, Chen J, et al. 2025. Genome-wide identification and expression profiling of bHLH transcription factors associated with ferulic acid biosynthesis in *Angelica sinensis*. *Frontiers in Plant Science* 16:1718585

[25] Zhang G, Jiao Y, Zhao Z, Chen Q, Wang Z, et al. 2024. Genome-wide and expression pattern analysis of the HIT4 gene family uncovers the involvement of *GHHIT4_4* in response to Verticillium Wilt in *Gossypium hirsutum*. *Genes* 15:348

[26] Zhao Y, Zhang G, Tang Q, Song W, Gao Q, et al. 2022. *EbMYBP1*, a R2R3-MYB transcription factor, promotes flavonoid biosynthesis in *Erigeron breviscapus*. *Frontiers in Plant Science* 13:946827

[27] Arshad KT, Xiang C, Yuan C, Li L, Wang J, et al. 2024. Elucidation of *AsANS* controlling pigment biosynthesis in *Angelica sinensis* through hormonal and transcriptomic analysis. *Physiologia Plantarum* 176:e14500

[28] Wang J, Zhou PH, Li CH, Liang YL, Liu GZ, et al. 2024. Progress on medicinal plant regeneration and the road ahead. *Medicinal Plant Biology* 3:e030

[29] Peng DQ, Luo MM, Guo XW, Li MF, Wei JH. 2024. Selection of reference genes for quantitative real-time PCR analysis in *Angelica sinensis*. *Chinese Traditional and Herbal Drugs* 55:269−278

[30] Luan Y, Chen Z, Meng J, Tao J, Zhao D. 2023. PoWRKY17 promotes drought tolerance in *Paeonia ostii* by modulating lignin accumulation. *Industrial Crops and Products* 204:117228

[31] Yuan C, Li L, Zhou P, Xiang C, Huang C, et al. 2025. Decoding the root lignification mechanism of *Angelica sinensis* through genome-wide DNA methylation analysis. *Journal of Experimental Botany* 76:2573−2589

[32] Chen S, Zhou Y, Chen Y, Gu J. 2018. Fastp: an ultra-fast all-in-one FASTQ preprocessor. *Bioinformatics* 34:i884−i890

[33] Kim D, Langmead B, Salzberg SL. 2015. HISAT: a fast spliced aligner with low memory requirements. *Nature Methods* 12:357−360

[34] Wang J, Li CH, Xiang CF, Zhou PH, Li LS, et al. 2024. Establishment and application of highly efficient regeneration, genetic transformation and genome editing system for cucurbitacins biosynthesis in *Hemsleya chinensis*. *BMC Plant Biology* 24:1052

[35] Zhang Q, Wang L, Wang Z, Zhang R, Liu P, et al. 2021. The regulation of cell wall lignification and lignin biosynthesis during pigmentation of winter jujube. *Horticulture Research* 8:238

[36] Li M, Cheng C, Zhang X, Zhou S, Wang C, et al. 2019. *PpNAC187* enhances lignin synthesis in 'Whangkeumbae' pear (*Pyrus pyrifolia*) 'Hard-End' fruit. *Molecules* 24:4338

[37] Jung SE, Kim TH, Shim JS, Bang SW, Bin Yoon H, et al. 2022. Rice *NAC17* transcription factor enhances drought tolerance by modulating lignin accumulation. *Plant Science* 323:111404

[38] Sun Y, Jiang C, Jiang R, Wang F, Zhang Z, et al. 2021. A novel NAC transcription factor from *Eucalyptus*, EgNAC141, positively regulates lignin biosynthesis and increases lignin deposition. *Frontiers in Plant Science* 12:642090

[39] Duan AQ, Tao JP, Jia LL, Tan GF, Liu JX, et al. 2020. AgNAC1, a celery transcription factor, related to regulation on lignin biosynthesis and salt tolerance. *Genomics* 112:5254−5264

[40] Nie G, Yang Z, He J, Liu A, Chen J, et al. 2021. Genome-wide investigation of the NAC transcription factor family in *Miscanthus sinensis* and expression analysis under various abiotic stresses. *Frontiers in Plant Science* 12:766550

[41] Ma M, Hao T, Ren X, Liu C, Gela A, et al. 2025. NAC family gene CmNAC34 positively regulates fruit ripening through interaction with CmNAC-NOR in *Cucumis melo*. *Journal of Integrative Agriculture* 24:2601−2618

[42] Xu Y, Zou S, Zeng H, Wang W, Wang B, et al. 2022. A NAC transcription factor TuNAC69 contributes to ANK-NLR-WRKY NLR-mediated stripe rust resistance in the diploid wheat *Triticum urartu*. *International Journal of Molecular Sciences* 23:564

[43] Li X, Wang N, She W, Guo Z, Pan H, et al. 2022. Identification and functional analysis of the *CgNAC043* gene involved in lignin synthesis from *Citrusgrandis* 'San Hong'. *Plants* 11:403

[44] Cheng C, Zhang C, Jin X, Wang T, Zhang Y, et al. 2025. Calcium disrupts CML38/WRKY46-NAC187-CCR cascade to inhibit the formation of lignin-related physiological disorders in pear fruit. *Plant Biotechnology Journal* 23:3478−3494

[45] Gong X, Qi K, Zhao L, Xie Z, Pan J, et al. 2024. PbAGL7–PbNAC47–PbMYB73 complex coordinately regulates *PbC3H1* and *PbHCT17* to promote the lignin biosynthesis in stone cells of pear fruit. *The Plant Journal* 120:1933−1953